nature genetics

Cooperative loss of RAS feedback regulation drives myeloid leukemogenesis

Zhen Zhao[1], Chi-Chao Chen[1,2], Cory D Rillahan[1], Ronglai Shen[3], Thomas Kitzing[1], Megan E McNerney[4], Ernesto Diaz-Flores[5], Johannes Zuber[6], Kevin Shannon[5], Michelle M Le Beau[7], Mona S Spector[8], Scott C Kogan[9,10] & Scott W Lowe[1,11]

RAS network activation is common in human cancers, and in acute myeloid leukemia (AML) this activation is achieved mainly through gain-of-function mutations in *KRAS*, *NRAS* or the receptor tyrosine kinase *FLT3*. We show that in mice, premalignant myeloid cells harboring a *Kras*^{G12D} allele retained low levels of Ras signaling owing to negative feedback involving Spry4 that prevented transformation. In humans, *SPRY4* is located on chromosome 5q, a region affected by large heterozygous deletions that are associated with aggressive disease in which gain-of-function mutations in the RAS pathway are rare. These 5q deletions often co-occur with chromosome 17 alterations involving the deletion of *NF1* (another RAS negative regulator) and *TP53*. Accordingly, combined suppression of Spry4, Nf1 and p53 produces high levels of Ras signaling and drives AML in mice. Thus, *SPRY4* is a tumor suppressor at 5q whose disruption contributes to a lethal AML subtype that appears to acquire RAS pathway activation through a loss of negative regulators.

AML is a heterogeneous cancer that represents the most common form of acute leukemia in adults[1]. Cytogenetic and molecular profiling of human AML samples has identified a range of missense mutations, translocations and large chromosomal events that can be associated with different patient outcomes[2,3]. Among the most common genetic events in AML are gain-of-function mutations in the RAS pathway, including activating mutations of *KRAS* and *NRAS* or of the upstream receptor tyrosine kinases *FLT3* and *KIT*[2,3]. Each of these mutations produces altered proteins that directly or indirectly drive RAS GTPase into a constitutively active GTP-bound state[4] and leads to constitutive activation of the mitogen-activated protein kinase (MAPK) and phosphoinositide 3-kinase (PI3K) pathways[4]. Although these lesions are considered important drivers of disease, *RAS* mutations alone are often unable to produce the high levels of MAPK and PI3K signaling necessary for malignant transformation without an increase in the copy number of mutant *KRAS* or *NRAS* or other mechanisms that enhance RAS output[5–7].

Previously, we found that activation of Kras via the *Kras*^{G12D} allele cooperates with RNA interference (RNAi)-mediated *Trp53* inactivation to induce AML in mice[8], and the AML cells had markedly elevated amounts of phosphorylated Erk (pErk; a MAPK effector) and S6 (pS6; an effector of both the MAPK and PI3K pathways) in both primary leukemia and transplanted secondary AML, even in the absence of stimulation by cytokine granulocyte-macrophage colony-stimulating factor (GM-CSF) (**Fig. 1a**,**b**)[8]. However, consistent with previous work[5,6,9,10], Kras G12D alone was unable to trigger a basal or cytokine-induced increase in the abundance of pErk or pS6 in bulk bone marrow cells, Kit$^+$ progenitors or Mac-1$^+$ mature myeloid cells as assessed by flow cytometry (**Fig. 1a**,**b** and **Supplementary Fig. 1a–d**). Thus, although highly activated Ras signaling appears to be an intrinsic feature of these AML cells, endogenous expression of oncogenic *Kras*^{G12D} is insufficient to sustain constitutive activation of downstream effectors in non-transformed myeloid cells. Although in some systems high pErk levels can be achieved via somatic duplication or amplification of the *Kras*^{G12D} allele[5,6], these events cannot explain the strong pathway activation that occurred in our AML model, as no increase in *Kras*^{G12D} allele balance[8] or corresponding protein levels was observed (**Supplementary Fig. 1e**).

It is well established that Ras activation can trigger compensatory feedback mechanisms that dampen signaling output[11–13]. To test whether such mechanisms might modulate Ras signaling during leukemogenesis, we generated wild-type or Kras G12D–expressing hematopoietic stem and progenitor cells (HSPCs) by transducing wild-type or Lox-Stop-Lox transcriptional silencing cassette (LSL)-*Kras*^{G12D} fetal liver cells with a vector encoding GFP-coupled, self-deleting Cre^{ER} (LGmCreER)[8]. After adding tamoxifen to induce Cre activity and thereby activate the *Kras*^{G12D} allele[8], we quantified the expression

[1]Cancer Biology and Genetics Program, Memorial Sloan-Kettering Cancer Center, New York, New York, USA. [2]Weill Cornell Graduate School of Medical Sciences, Cornell University, New York, New York, USA. [3]Department of Epidemiology and Biostatistics, Memorial Sloan-Kettering Cancer Center, New York, New York, USA. [4]Department of Pathology, Department of Pediatrics, Section of Hematology/Oncology, University of Chicago, Chicago, Illinois, USA. [5]Department of Pediatrics, University of California, San Francisco, San Francisco, California, USA. [6]Research Institute of Molecular Pathology (IMP), Vienna Biocenter (VBC), Vienna, Austria. [7]Department of Medicine, Section of Hematology/Oncology, University of Chicago, Chicago, Illinois, USA. [8]Cold Spring Harbor Laboratory, Cold Spring Harbor, New York, USA. [9]Department of Laboratory Medicine, University of California, San Francisco, San Francisco, California, USA. [10]Department of Laboratory Medicine and Helen Diller Family Comprehensive Cancer Center, University of California, San Francisco, San Francisco, California, USA. [11]Howard Hughes Medical Institute, New York, New York, USA. Correspondence should be addressed to S.W.L. (lowes@mskcc.org).

Received 24 October 2014; accepted 24 February 2015; published online 30 March 2015; doi:10.1038/ng.3251

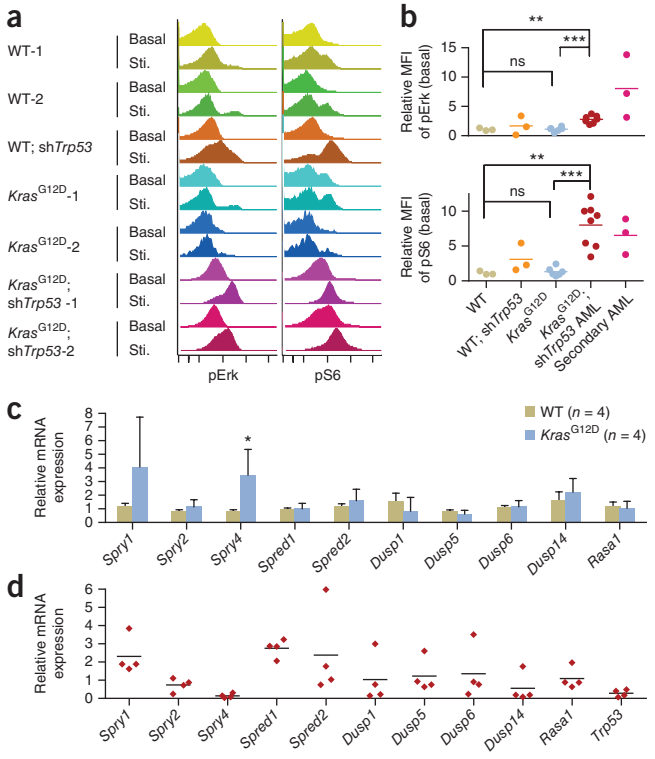

Figure 1 Reduced *Spry4* expression correlates with increases in Ras signaling during Kras G12D–induced leukemogenesis. (**a**) Representative phosphosignaling analysis (phospho-FACS) showing that basal and cytokine-responsive (GM-CSF stimulation (Sti.)) pErk and pS6 levels were enhanced in *Kras*^{G12D} leukemia cells with *Trp53* knockdown (*Kras*^{G12D}; sh*Trp53*) relative to those in non-leukemic bone marrow cells derived from wild-type (WT) mice, mice with wild-type *Kras* and *Trp53* knockdown (WT; sh*Trp53*) or *Kras*^{G12D} mice. (**b**) Quantification of basal mean fluorescence intensity (MFI) of pErk (top) and pS6 (bottom) showing significant elevation of signaling in primary and secondary leukemia. Relative MFI was calculated by dividing the MFI of GFP$^+$ (LGmCreER) infected cells by the MFI of GFP$^-$ uninfected cells from the same mouse. Data were derived from primary recipient mice transplanted with independently generated and infected HSPCs (n = 3–8 in each group; $^{**}P < 0.01$, $^{***}P < 0.001$ via two-tailed t-test, with Welch's correction when applicable). ns, not significant. (**c**) Results of qRT-PCR analyses showing significant induction of *Spry4* upon Kras G12D activation in HSPCs. Data were derived from two experiments using independently generated and infected HSPCs (n = 4; $^{*}P < 0.05$ via two-way repeated-measures analysis of variance (ANOVA); the bar graph shows mean + s.d.). (**d**) Results of qRT-PCR analyses showing RNA expression of the same genes as in **c** in *Kras*^{G12D} leukemia cells with *Trp53* knockdown relative to that in normal bone marrow cells (normalized to 1 for all genes). Note the suppression of *Trp53* and *Spry4* in all independently derived primary samples (n = 4, Column Statistics).

of ten known Ras negative-feedback genes[11] in GFP$^+$ cells expressing myeloid markers (**Supplementary Fig. 1f**). Quantitative RT-PCR (qRT-PCR) analysis showed that *Spry4* was significantly upregulated by mutant Kras expression (**Fig. 1c**) but underexpressed in *Kras*^{G12D} leukemia cells with knockdown of *Trp53* compared to normal bone marrow cells (**Fig. 1d**).

The inverse correlation between *Spry4* expression and Ras effector pathway activation was particularly interesting given the role of Sprouty proteins as negative regulators of Ras-MAPK signaling during development[14]. To test whether Spry4-mediated feedback limits Ras-induced leukemogenesis, we used the established transplantation-based approach to assess the effect of Spry4 suppression on *Kras*^{G12D}-induced leukemogenesis[8,15]. In this approach, control and *Spry4* short hairpin RNAs (shRNAs) (**Supplementary Fig. 2a**,**b**) were transduced into LSL-*Kras*^{G12D} HSPCs using the LGmCreER vector, and the resulting cells were treated with tamoxifen to activate *Kras*^{G12D}. Mice receiving HSPCs transduced with each of three *Spry4* shRNAs displayed accelerated onset of T cell lymphoma driven by oncogenic *Kras*[16,17] (**Supplementary Fig. 2b**). Thus, Spry4 suppression cooperated with Kras G12D activation during tumorigenesis.

To assess whether Spry4 can also limit the development of myeloid neoplasia, we biased the system against lymphoid disease by using C57BL/6J athymic mice (*Foxn1*^{nu}) as recipients. In these studies, we transduced two of the validated *Spry4* shRNAs into LSL-*Kras*^{G12D}; *Trp53*$^{+/-}$ HSPCs, anticipating loss of the wild-type *Trp53* allele during leukemogenesis. Again, both *Spry4* shRNAs accelerated disease onset (**Fig. 2a**) (median survival of 112 and 215 d for recipients of *Kras*^{G12D}; *Trp53*$^{+/-}$ HSPCs with knockdown of *Spry4* (KP-S HSPCs) and *Kras*^{G12D}; *Trp53*$^{+/-}$ HSPCs with knockdown by a control shRNA (KP-C HSPCs), respectively; $P < 0.01$). Interestingly, *Trp53* remained intact in both KP-S and KP-C malignancies, which suggests that p53 can function as a haploinsufficient tumor suppressor in this model (**Supplementary Fig. 2c**). Histopathological analyses of moribund animals showed that all KP-S and KP-C recipient mice developed histiocytic sarcoma, an aggressive tumor of monocyte-derived cells that manifests in spleen and liver (**Fig. 2b** and **Supplementary Fig. 3a**). Flow cytometry indicated that the spleens of KP-S recipients were massively enriched for cells expressing intermediate amounts of the myeloid marker Mac-1 (**Fig. 2c**) and that these cells showed elevated amounts of both pErk and pS6, with elevation exacerbated by serum stimulation (**Fig. 2c**). Notably, neoplastic cells isolated from two independent KP-S mice induced secondary disease in sublethally irradiated recipient mice at 100% penetrance (**Supplementary Fig. 3b**). These results demonstrate that *Spry4* knockdown accelerates oncogenesis and potentiates Kras-mediated myeloid transformation by increasing Ras signaling output.

In humans, *SPRY4* is located at chromosome 5q31.3 and is frequently deleted in the context of del(5q) in patients with myelodysplastic syndrome (MDS), complex-karyotype AML and therapy-related myeloid neoplasms (t-MNs)[18–20]. Analysis of data from The Cancer Genome Atlas (TCGA)[2,21,22] showed that *SPRY4* was deleted in 17 of 187 patients with AML (9% overall deletion rate) as part of chromosome 5q (**Fig. 3a**). These findings were confirmed in a separate cohort of 35 subjects with AML or t-MNs. Here *SPRY4* deletion, defined by SNP array analysis, was found in 12 of 13 samples with karyotyping-confirmed 5q abnormalities, as well as in one other sample with unknown cytogenetic information (**Fig. 3a**). These observations, together with our functional studies, suggest a role for *SPRY4* in human leukemia.

Although the action of oncogenic Kras and suppression of Spry4 can cooperate during tumorigenesis, *KRAS* and *NRAS* mutations rarely occur in human del(5q) AML[23,24]. Indeed, whereas 42% of human AML samples show gain-of-function RAS pathway mutations (*KRAS*, *NRAS*, *FLT3* and/or *KIT*), such mutations were significantly under-represented in individuals with del(5q) AML harboring *SPRY4* deletion (only 3 of 17; Fisher's exact test, $P = 0.025$). Instead, *SPRY4*-encompassing del(5q) often co-occurred with *TP53* mutations and/or deletion of the *TP53* locus on chromosome 17p (**Fig. 3b** and **Supplementary Figs. 4** and **5a**,**b**; $P < 0.0005$). In addition to deletion of *SPRY4*, del(5q) AML frequently harbors losses of other negative RAS regulators, including *RASA1* (encoding p120-RasGAP; 5q), *DUSP1* (5q), *DUSP14* (17q) and *NF1* (17q) (**Fig. 3b** and **Supplementary Figs. 4** and **5**; odds ratio > 10, $P < 0.0005$ for

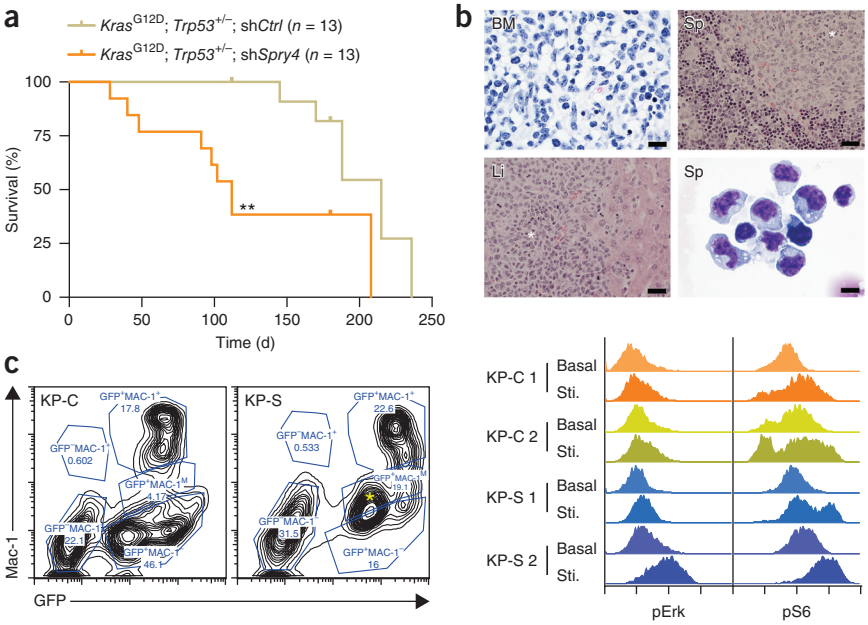

Figure 2 *Spry4* knockdown accelerates leukemogenesis. (**a**) Kaplan-Meier curve of overall survival of athymic mice reconstituted with *Kras*^{G12D}; *Trp53*$^{+/-}$ HSPCs with *Spry4* knockdown (KP-S) in comparison with that of recipients of these HSPCs expressing control shRNA (KP-C). Data were derived from two independent experiments using independently generated and infected HSPCs (** $P < 0.01$). (**b**) Representative histopathology of KP-S histiocytic sarcomas: malignant cells were present in the bone marrow (BM), liver (Li) and spleen (Sp) (asterisks indicate histiocytes), as shown by hematoxylin and eosin staining. Spleen included numerous cells with a monocytic to histiocytic appearance after cytospin and Wright-Giemsa staining (bottom right panel). Scale bars represent 12 μm for BM (100×), 30 μm for liver and spleen (40×) and 8 μm for spleen cytospin (100×). (**c**) Left, results of flow cytometry analyses showing expansion of the Mac-1 intermediate population (GFP^{+}Mac-1^{M}) in spleens of KP-S recipients (population marked with an asterisk). Also shown are gating strategies based on the level of Mac-1 expression (GFP^{+}Mac-1^{+}, GFP^{-}Mac-1^{+}, GFP^{+}Mac-1^{M}, GFP^{-}Mac-1^{-} and GFP^{+}Mac-1^{-}). Right, representative phospho-FACS analyses showing basal and serum-responsive (Sti.) pErk and pS6 levels of malignant histiocytic sarcoma cells derived from KP-S and KP-C mice. KP-S recipients showed enhanced responsive pErk and pS6 levels in the GFP^{+}Mac-1^{M} population compared with the same cell population in KP-C mice. Data were from independent primary histiocytic sarcomas induced by independently generated and infected HSPCs (n = 2–3 in each group).

all combinations by cBioPortal; see URLs). Interestingly, analysis of transcriptional profiles showed significant overlap between gene ontology categories enriched in AML with *SPRY4*-encompassing 5q deletion and those enriched in *NRAS*-mutant AML (six overlapping pathways: five downregulated and one upregulated; $P = 1.7 \times 10^{-5}$) (**Supplementary Fig. 6a**). In addition, these del(5q) AMLs with *SPRY4* loss displayed a gene set enrichment signature and a global gene expression pattern similar to that of AML harboring *NRAS* or *KRAS* mutations (**Supplementary Fig. 6b**,**c**). These results suggest that del(5q) AML may acquire RAS pathway activation through the combined loss of negative regulators, rather than through mutational activation of a single pathway component.

We next tested whether combined inhibition of Ras negative regulators could drive AML in the absence of an activated *Ras* allele. Given the significant co-occurrence of *SPRY4*, *NF1* and *TP53* deletions in del(5q) AML ($P < 0.0001$; **Supplementary Fig. 5b**), we chose to cosuppress *Spry4* and *Nf1* in a *Trp53*-null background using the HSPC transduction and transplantation system described above. In this iteration, we knocked down either *Nf1* (*Nf1* shRNA–mCherry) or *Spry4* (*Spry4* shRNA–GFP) along with *Renilla* luciferase (Ren) (control shRNA coupled to a molecule of the opposite color[25]), or we knocked down expression of these genes in combination in *Trp53*$^{-/-}$ HSPCs (experimental design shown in **Fig. 4a**). Interestingly, suppression of *Nf1* alone led to the upregulation of *Spry4* and vice versa (**Supplementary Fig. 7a**), suggesting a mutual compensatory process that accounts for the co-occurring deletions of multiple genes in this pathway. Accordingly, the abundance of pErk and pS6 was significantly increased in

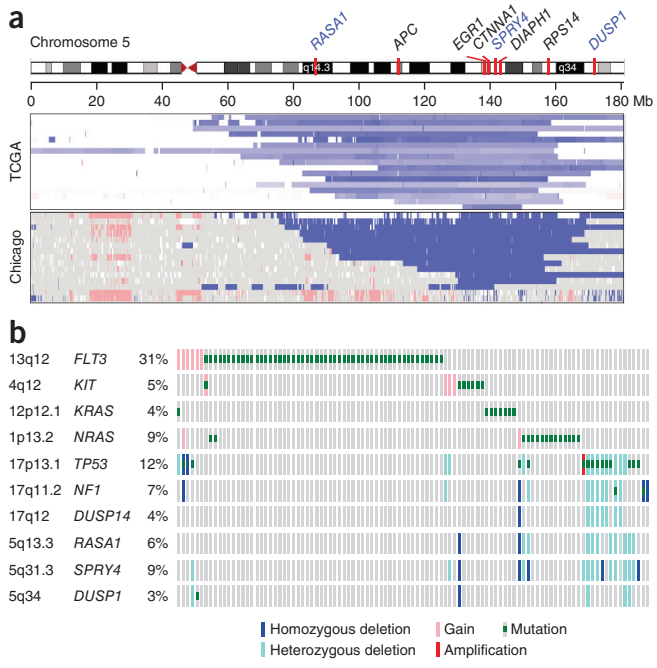

Figure 3 *SPRY4* and other negative regulators of the RAS pathway are deleted in del(5q) AML. (**a**) Top, chromosome 5 copy number analysis of subjects with AML published within the TCGA AML data set. Deletions (purple) involving various regions of chromosome 5q included *SPRY4* in 17 samples. Bottom, in a set of 35 patients (Chicago data set) with *de novo* AML or t-MN analyzed by SNP array, 13 samples exhibited deletion of *SPRY4* (among 15 samples shown, 13 samples had –5/del(5q) as detected by cytogenetic analysis, of which 12 showed *SPRY4* deletions; there was 1 additional *SPRY4*-deleted sample without cytogenetic information). (**b**) Putative copy number alterations in the TCGA data set showing deletion of negative-feedback regulatory genes on 5q and 17q, in the context of mutation and/or deletion of *TP53*. Notably, these cases lack mutation and/or amplification in *FLT3*, *KIT* and *RAS*. The genomic location and alteration frequency of all genes is shown on the left. For clarity, only the 103 cases that had the abovementioned alterations (among a total of 187 cases) are shown (cBioPortal; see URLs).

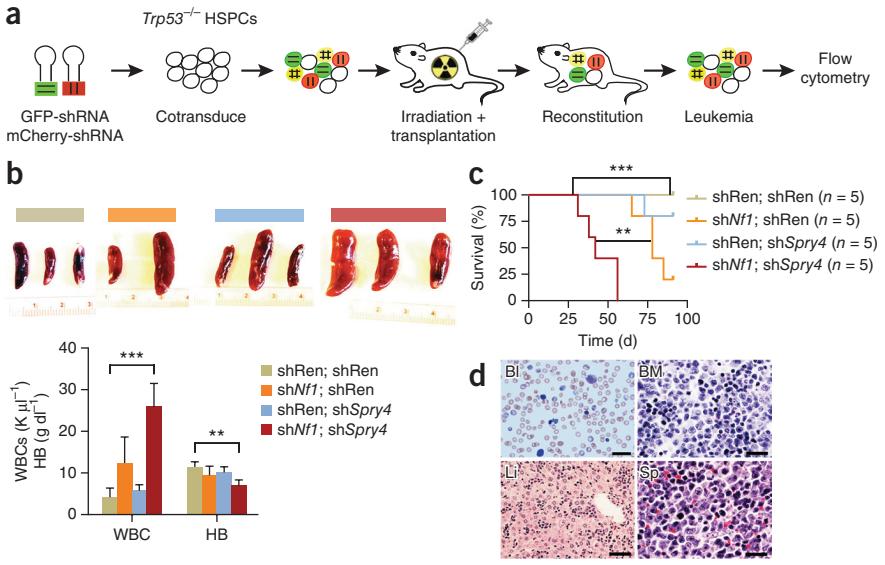

Figure 4 The combined suppression of Spry4 and Nf1 promotes myeloid leukemogenesis. (**a**) Schematic showing the experimental design for testing the cooperation between Spry4 and Nf1 suppression on a background of *Trp53* deficiency. Combinations tested were double knockdown of *Renilla* luciferase (shRen; shRen), double knockdown of *Nf1* and *Renilla* luciferase (sh*Nf1*; shRen), double knockdown of *Renilla* luciferase and *Spry4* (shRen; sh*Spry4*) and double knockdown of *Nf1* and *Spry4* (sh*Nf1*; sh*Spry4*) (mCherry; GFP). (**b**) Splenomegaly was consistently found in mice reconstituted with *Trp53*$^{-/-}$; sh*Nf1*; sh*Spry4* HSPCs after 5 weeks. Peripheral blood analyses of *Trp53*$^{-/-}$; sh*Nf1*; sh*Spry4* recipient mice at 8 weeks showed elevated white blood cell (WBC) counts and reduced levels of hemoglobin (HB) (n = 2–5 in each group; $^{**}P < 0.01$, $^{***}P < 0.0001$ via two-tailed t-test; the bar graph shows mean + s.d.). K, 1,000 cells. (**c**) Kaplan-Meier curves showing that mice reconstituted with *Trp53*$^{-/-}$; sh*Nf1*; sh*Spry4* HSPCs had significantly reduced overall survival (n = 5 in all groups; $^{**}P < 0.01$, $^{***}P < 0.0001$). (**d**) Histopathology analysis showing leukemia in peripheral blood (Bl), bone marrow (BM), liver (Li) and spleen (Sp) after hematoxylin and eosin staining. Scale bars represent 20 μm for BM and Sp (100×), 50 μm for Li (40×) and 33 μm for Bl (60×).

premalignant cells with double knockdown of *Nf1* and *Spry4* compared to that in cells with *Nf1* knockdown only, indicating that *Spry4* contributes to negative feedback when Ras signaling is deregulated (**Supplementary Fig. 7b**).

Thymectomized mice transplanted with *Trp53*$^{-/-}$ HSPCs transduced with constructs for *Nf1* and *Spry4* shRNAs (*Trp53*$^{-/-}$; sh*Nf1*; sh*Spry4* HSPCs) displayed accelerated leukemia onset compared with mice transplanted with any of the controls (**Fig. 4b–d** and **Supplementary Fig. 8a**). The moribund mice harboring these cells presented with splenomegaly, increased white blood cell counts and anemia (**Fig. 4b**), leading to reduced overall survival (**Fig. 4c**; median survival of 42 d in recipients of cells with double knockdown of *Nf1* and *Spry4* compared to 78 d in recipients of cells with *Nf1* knockdown only; $P < 0.0001$ versus control Ren shRNA, $P = 0.0027$ versus *Nf1* shRNA). As expected, these *Trp53*$^{-/-}$; sh*Nf1*; sh*Spry4* leukemia cells displayed high levels of Ras signaling (**Supplementary Fig. 8b**). Histopathological analyses indicated that these animals displayed leukemic blasts in the peripheral blood, that their bone marrow and spleens had disrupted architecture, and that leukemia cells had disseminated into the liver and spleen (**Fig. 4d**). Leukemic cells expressed modest levels of Gr-1, Mac-1 and Ter-119 but lacked expression of B220 and CD3ε, and they had an increased proportion of Lin^{-}Kit^{+} myeloid progenitors, consistent with an immature myeloid phenotype (**Supplementary Fig. 9a**,**b**). Leukemic cells isolated from both bone marrow and spleen produced secondary malignancies identical to the primary disease when transplanted into sublethally irradiated recipients, whereas *Trp53*$^{-/-}$ cells with *Nf1* knockdown failed to do so within the same time frame (data not shown). Thus, co-suppression of Spry4 and Nf1 acts in a p53-deficient background to produce AML of an early hematopoietic phenotype with myeloid maturation.

The studies described above functionally validate a new tumor suppressor in del(5q) AML and, in doing so, provide insights into its etiology. Although *CSNK1A1*, *RPS14*, *EGR1* and *APC* have been implicated as putative tumor suppressors on 5q, the mechanism(s) by which alterations in each contribute to leukemogenesis alone or in combination are not completely understood[26–29]. Our finding that *SPRY4* is frequently deleted together with other negative regulators of RAS signaling suggests that one way del(5q) can contribute to leukemogenesis is by augmenting flux through the RAS pathway. The lack of frequent mutation or silencing of the remaining allele for any gene in del(5q) deletions implies that tumor suppressors in this region are haploinsufficient[28,29]. Accordingly, we found that the levels of *Spry4* mRNA in *Spry4*-knockdown leukemia were halved (**Supplementary Fig. 8c**). These findings are consistent with the emerging view that large chromosomal deletions contain multiple haploinsufficient tumor suppressors whose attenuation can functionally cooperate during tumorigenesis[30–32].

In addition, our results suggest a mechanism for RAS pathway activation in del(5q) AML that may have broader relevance. In contrast to other AML subtypes in which RAS signaling is activated by mutation of the *NRAS*, *KRAS* or *FLT3* oncogenes, del(5q) AML cells harbor losses of multiple RAS signaling negative regulatory genes that can functionally cooperate to achieve high levels of RAS pathway activation. The loss of multiple negative regulators may be necessary given the typically less potent induction of RAS activation by negative regulator loss[33]. In addition to *SPRY4* and *NF1*, *RASA1* (5q13), *DUSP1* (5q34) and *DUSP14* (17q12) are also frequently deleted in del(5q) AML and may have an important role in human disease progression. Previous work in lymphoma provides support for this model of tumor suppression, where combined haploinsufficiencies of genes in the same pathway, rather than two 'hits' in a single gene, can promote tumorigenesis[25]. Interestingly, we noted that additional cancer types with low rates of activating mutations in the RAS pathway, such as prostate adenocarcinoma (TCGA, provisional)[21,22] and glioblastoma[34], may contain deletions of multiple negative regulators that, in principle, may contribute to pathway activation in these tumor types (heterozygous and homozygous deletions of RAS negative regulators seen in 46.1% and 97.2% of cases, respectively). Thus a more thorough investigation of the functional consequences of these deletions is clearly warranted, particularly given that this could broaden patient stratification for RAS pathway–targeted therapies.

URLs. cBioPortal, tumor data case set, http://www.cbioportal.org/index.do?cancer_study_id=laml_tcga&genetic_profile_ids_PROFILE_MUTATION_EXTENDED=laml_tcga_mutations&genetic_profile_ids_PROFILE_COPY_NUMBER_ALTERATION=laml_tcga_gistic&Z_SCORE_THRESHOLD=2.0&data_priority=0&case_set_id=laml_tcga_cnaseq&case_ids=&gene_set_choice=user-defined-list&gene_list=FLT3%3AGAIN%2CAMP%2CMUT%3B%0D%0AKIT%3AGAIN%2CAMP%2CMUT%3B%0D%0AKRAS%3AGAIN%2CAMP%2CMUT%3B%0D%0ANRAS%3AGAIN%2CAMP%2CMUT%3B%0D%0ATP53%3AAMP%2CMUT%2CHOMDEL%2CHETLOSS%3B%0D%0ANF1%3AMUT%2CHOMDEL%2C+HETLOSS%3B%0D%0ADUSP14%3AMUT%2CHOMDEL%2C+HETLOSS%3B%0D%0ARASA1%3AMUT%2CHOMDEL%2C+HETLOSS%3B%0D%0ASPRY4%3AMUT%2CHOMDEL%2C+HETLOSS%3B%0D%0ADUSP1%3AMUT%2CHOMDEL%2C+HETLOSS%3B&clinical_param_selection=null&tab_index=tab_visualize&Action=Submit; TCGA Data Portal case counts for AML, https://tcga-data.nci.nih.gov/tcga/tcgaCancerDetails.jsp?diseaseType=LAML&diseaseName=Acute%20Myeloid%20Leukemia; Jackson Laboratory, http://www.jax.org/index.html.

METHODS

Methods and any associated references are available in the online version of the paper.

Note: Any Supplementary Information and Source Data files are available in the online version of the paper.

ACKNOWLEDGMENTS

The authors gratefully acknowledge A. Chicas, O. Aksoy, C.-H. Huang, C. He and C. Chen for their expert technical assistance, advice and supportive data, as well as members of the Lowe laboratory for helpful comments. The authors also thank C. Sherr and S. Mayack for editorial comments on the manuscript. This study was supported by a Specialized Center of Research (SCOR) grant from the Leukemia & Lymphoma Society (LLS), a Starr Cancer Consortium grant, the Don Monti Memorial Research Foundation, the Geoffrey Beene Center for Cancer Research, an Award from the Ministry of Education of Taiwan to C.-C.C. and an LLS Research Fellow Award to C.D.R. (5428-15). S.W.L. is an investigator in the Howard Hughes Medical Institute.

AUTHOR CONTRIBUTIONS

Z.Z. designed, carried out and analyzed the experiments. C.-C.C. cloned miRE shRNA and carried out gene set enrichment analysis. C.-C.C. and R.S. analyzed expression patterns of TCGA data and carried out statistical analysis for all bioinformatics results. M.E.M. and M.M.L.B. provided RNA-seq, SNP array and partial karyotyping data for 35 patients from the University of Chicago. T.K. analyzed the cBioPortal database. *In vivo* phospho-FACS experiments were done by Z.Z. and E.D.-F. with suggestions from K.S. J.Z. cloned *Spry4* shRNA–related constructs and suggested *in vivo* experiments. M.S.S. analyzed deletion and mutational data for *SPRY4*, cloned *Spry4* cDNA, proposed experiments and revised the manuscript. S.C.K. characterized the phenotype and immunophenotype of models and helped to design experiments. S.W.L. designed and analyzed experiments and supervised the work. Z.Z., C.D.R. and S.W.L. wrote the paper.

COMPETING FINANCIAL INTERESTS

The authors declare no competing financial interests.

1. Bullinger, L. *et al.* Use of gene-expression profiling to identify prognostic subclasses in adult acute myeloid leukemia. *N. Engl. J. Med.* **350**, 1605–1616 (2004).
2. Cancer Genome Atlas Research Network Genomic and epigenomic landscapes of adult *de novo* acute myeloid leukemia. *N. Engl. J. Med.* **368**, 2059–2074 (2013).
3. Patel, J.P. *et al.* Prognostic relevance of integrated genetic profiling in acute myeloid leukemia. *N. Engl. J. Med.* **366**, 1079–1089 (2012).
4. Schubbert, S., Shannon, K. & Bollag, G. Hyperactive Ras in developmental disorders and cancer. *Nat. Rev. Cancer* **7**, 295–308 (2007).
5. Feldser, D.M. *et al.* Stage-specific sensitivity to p53 restoration during lung cancer progression. *Nature* **468**, 572–575 (2010).
6. Junttila, M.R. *et al.* Selective activation of p53-mediated tumour suppression in high-grade tumours. *Nature* **468**, 567–571 (2010).
7. Xu, J. *et al.* Dominant role of oncogene dosage and absence of tumor suppressor activity in *Nras*-driven hematopoietic transformation. *Cancer Discov.* **3**, 993–1001 (2013).
8. Zhao, Z. *et al.* p53 loss promotes acute myeloid leukemia by enabling aberrant self-renewal. *Genes Dev.* **24**, 1389–1402 (2010).
9. Braun, B.S. *et al.* Somatic activation of oncogenic *Kras* in hematopoietic cells initiates a rapidly fatal myeloproliferative disorder. *Proc. Natl. Acad. Sci. USA* **101**, 597–602 (2004).
10. Van Meter, M.E. *et al.* K-RasG12D expression induces hyperproliferation and aberrant signaling in primary hematopoietic stem/progenitor cells. *Blood* **109**, 3945–3952 (2007).
11. Courtois-Cox, S. *et al.* A negative feedback signaling network underlies oncogene-induced senescence. *Cancer Cell* **10**, 459–472 (2006).
12. Xue, W. *et al.* Senescence and tumour clearance is triggered by p53 restoration in murine liver carcinomas. *Nature* **445**, 656–660 (2007).
13. Chicas, A. *et al.* Dissecting the unique role of the retinoblastoma tumor suppressor during cellular senescence. *Cancer Cell* **17**, 376–387 (2010).
14. Kim, H.J. & Bar-Sagi, D. Modulation of signalling by Sprouty: a developing story. *Nat. Rev. Mol. Cell Biol.* **5**, 441–450 (2004).
15. Chen, C. *et al.* MLL3 is a haploinsufficient 7q tumor suppressor in acute myeloid leukemia. *Cancer Cell* **25**, 652–665 (2014).
16. Zhang, J. *et al.* Oncogenic *Kras*-induced leukemogenesis: hematopoietic stem cells as the initial target and lineage-specific progenitors as the potential targets for final leukemic transformation. *Blood* **113**, 1304–1314 (2009).
17. Sabnis, A.J. *et al.* Oncogenic *Kras* initiates leukemia in hematopoietic stem cells. *PLoS Biol.* **7**, e59 (2009).
18. Douet-Guilbert, N. *et al.* Molecular characterization of deletions of the long arm of chromosome 5 (del(5q)) in 94 MDS/AML patients. *Leukemia* **26**, 1695–1697 (2012).
19. Zhao, N. *et al.* Molecular delineation of the smallest commonly deleted region of chromosome 5 in malignant myeloid diseases to 1–1.5 Mb and preparation of a PAC-based physical map. *Proc. Natl. Acad. Sci. USA* **94**, 6948–6953 (1997).
20. Jerez, A. *et al.* Topography, clinical, and genomic correlates of 5q myeloid malignancies revisited. *J. Clin. Oncol.* **30**, 1343–1349 (2012).
21. Cerami, E. *et al.* The cBio cancer genomics portal: an open platform for exploring multidimensional cancer genomics data. *Cancer Discov.* **2**, 401–404 (2012).
22. Gao, J. *et al.* Integrative analysis of complex cancer genomics and clinical profiles using the cBioPortal. *Sci. Signal.* **6**, pl1 (2013).
23. Bowen, D.T. *et al. RAS* mutation in acute myeloid leukemia is associated with distinct cytogenetic subgroups but does not influence outcome in patients younger than 60 years. *Blood* **106**, 2113–2119 (2005).
24. Kadia, T.M. *et al.* Clinical and proteomic characterization of acute myeloid leukemia with mutated *RAS*. *Cancer* **118**, 5550–5559 (2012).
25. Scuoppo, C. *et al.* A tumour suppressor network relying on the polyamine-hypusine axis. *Nature* **487**, 244–248 (2012).
26. Schneider, R.K. *et al.* Role of casein kinase 1A1 in the biology and targeted therapy of del(5q) MDS. *Cancer Cell* **26**, 509–520 (2014).
27. Ebert, B.L. *et al.* Identification of *RPS14* as a 5q$^-$ syndrome gene by RNA interference screen. *Nature* **451**, 335–339 (2008).
28. Joslin, J.M. *et al.* Haploinsufficiency of *EGR1*, a candidate gene in the del(5q), leads to the development of myeloid disorders. *Blood* **110**, 719–726 (2007).
29. Wang, J., Fernald, A.A., Anastasi, J., Le Beau, M.M. & Qian, Z. Haploinsufficiency of *Apc* leads to ineffective hematopoiesis. *Blood* **115**, 3481–3488 (2010).
30. Xue, W. *et al.* A cluster of cooperating tumor-suppressor gene candidates in chromosomal deletions. *Proc. Natl. Acad. Sci. USA* **109**, 8212–8217 (2012).
31. Davoli, T. *et al.* Cumulative haploinsufficiency and triplosensitivity drive aneuploidy patterns and shape the cancer genome. *Cell* **155**, 948–962 (2013).
32. Solimini, N.L. *et al.* Recurrent hemizygous deletions in cancers may optimize proliferative potential. *Science* **337**, 104–109 (2012).
33. Cutts, B.A. *et al. Nf1* deficiency cooperates with oncogenic K-RAS to induce acute myeloid leukemia in mice. *Blood* **114**, 3629–3632 (2009).
34. Brennan, C.W. *et al.* The somatic genomic landscape of glioblastoma. *Cell* **155**, 462–477 (2013).

ONLINE METHODS

Retroviral constructs. LMP, LGmCreER and LMS vectors have been described previously[8,35]. miR30 shRNAs targeting mouse orthologs of the *Spry4* gene were designed using DSIR, PCR amplified from 97-mer oligonucleotides using specific primers, digested with XhoI and EcoRI, cloned into predigested MSCV-miR30-PGK-Puromycin (LMP), MSCV-GFP-miR30-PGK-Cre (LGmCreER) or MSCV-miRE-SV40-GFP/mCherry (LMS) retroviral vectors, and sequence verified as previously described[36,37]. LMP constructs were used for testing the knockdown efficiency of *Spry4* shRNA in NIH 3T3 cells; LGmCreER constructs were used in LSL-*Kras*^{G12D} and LSL-*Kras*^{G12D}; *Trp53*$^{+/-}$ HSPCs to introduce both self-deleting Cre^{ER} and *Spry4* shRNA; and LMS constructs were used in *Trp53*$^{-/-}$ HSPCs to introduce *Spry4* shRNA and *Nf1* shRNA independently. All shRNA guide sequences are listed in **Supplementary Table 1**.

Mouse strains. All mouse strain–related experiments were done with the approval of the Cold Spring Harbor Laboratory Animal Care and Use Committee and/or the Memorial Sloan Kettering Cancer Center (MSKCC) Institutional Animal Care and Use Committees. LSL-*Kras*^{G12D} and *Trp53*$^{-/-}$ mice were backcrossed onto the C57BL/6 background for more than six generations. Genotyping was done according to standard protocols available at http://mouse.ncifcrf.gov/. Syngeneic C57BL/6 mice (Charles River) were recipients in the transplantation experiment using LSL-*Kras*^{G12D} HSPCs with *Spry4* knockdown shown in **Supplementary Figure 2b**. B6.Cg-Foxn1nu/J mice were purchased from the Jackson Laboratory (000819) and used as recipients in LSL-*Kras*^{G12D}; *Trp53*$^{+/-}$ HSPC transplantation experiments (**Fig. 2**), and thymectomized C57BL/6 mice were purchased from Jackson Laboratory and used as recipients in the *Trp53*$^{-/-}$; sh*Nf1*; sh*Spry4* HSPC transplantation experiments (**Fig. 4**).

HSPC isolation, retroviral transduction and transplantation. HSPC isolation and retroviral transduction were carried out as described previously[8]. In brief, day 13.5–15.5 fetal liver cells of wild-type, LSL-*Kras*^{G12D}, *Trp53*$^{-/-}$ and LSL-*Kras*^{G12D}; *Trp53*$^{+/-}$ strains were collected. LGmCreER retroviral constructs encoding GFP-coupled self-deleting Cre^{ER} and the shRNAs described above were used in wild-type, LSL-*Kras*^{G12D} and LSL-*Kras*^{G12D}; *Trp53*$^{+/-}$ cells to introduce both Cre and the desired shRNA. For knockdown of *Spry4* in LSL-*Kras*^{G12D} cells, three shRNAs targeting *Spry4* were used individually. For knockdown of *Spry4* in LSL-*Kras*^{G12D}; *Trp53*$^{+/-}$ cells, *Spry4*.1865 shRNA and *Spry4*.2344 shRNA were used individually. Cosuppression of Nf1 and Spry4 was done by coinfecting *Trp53*$^{-/-}$ HSPCs with an miRE-based MLS retroviral construct containing *Nf1*(mCherry) shRNA and three pooled shRNAs targeting *Spry4*(GFP). To induce Cre activity *in vitro*, we treated infected HSPCs with 0.2 μM 4-OHT (Sigma-Aldrich; dissolved in 95% cold ethanol) for 36–48 h. Approximately 2×10^6 cells were injected into the tail veins of 8- to 10-week-old lethally irradiated syngeneic C57BL/6 mice (8.2 Gy total in a single dose), 10-week-old lethally irradiated B6.Cg-Foxn1nu/J mice (6.5 Gy total in a single dose) or 10-week-old lethally irradiated thymectomized C57BL/6 mice (7.5 Gy total in a single dose) (Gammacell 40 Exactor, MDS Nordion). For secondary leukemia transplantation, ~1×10^6 leukemia cells isolated from bone marrow or spleen were transplanted into sublethally irradiated syngeneic C57BL/6 recipient mice (4.5 Gy in a single dose).

Quantitative RT-PCR analysis. To analyze the induction of negative-feedback regulators by the expression of oncogenic *Kras*, we infected wild-type and LSL-*Kras*^{G12D} fetal liver–derived HSPCs with LGmCreER without shRNA, and *Kras*^{G12D} was activated for 48 h as described above followed by 5 d in culture in the presence of cytokines as described[38]. GFP$^+$ transduced cells were sorted before RNA extraction. Total RNA was isolated using the RNeasy Mini Kit (Qiagen) and converted to cDNA using TaqMan Reverse Transcription reagents (Applied Biosystems). Gene-specific primer sets were designed using Primer Express 1.5. qRT-PCR was carried out in triplicate using SYBR Green PCR Master Mix (Applied Biosystems) on a Roche IQ5 ICycler. *Gapdh* or *Actb* served as an endogenous control, and all quantification was done using the ΔC_t method.

For assessment of *in vitro* target-gene knockdown, *Trp53*$^{-/-}$ HSPCs were coinfected with one of four shRNA combinations: Ren shRNA; Ren shRNA, *Nf1* shRNA; Ren shRNA, Ren shRNA; *Spry4* shRNA or *Nf1* shRNA; *Spry4* shRNA (all in sequence of mCherry; GFP). Cells were grown for 4 d, and the mCherry-GFP double-positive cells from all combinations were then sorted for RNA isolation and qRT-PCR analysis. For *in vivo Spry4* knockdown, mCherry-GFP double-positive *Trp53*$^{-/-}$; sh*Nf1*; sh*Spry4* leukemias were sorted and compared to mCherry-positive *Trp53*$^{-/-}$ leukemias with *Nf1* knockdown only that eventually grew from the (*Nf1* shRNA–mCherry)–(Ren shRNA–GFP) transplant shown in **Figure 4**. qPCR primers are listed in **Supplementary Table 2**.

Histocytological and molecular characterization of myeloid malignancy. Peripheral blood was obtained from recipient mice during leukemogenesis and at the terminal disease stage, and blood smears were stained with Wright-Giemsa stain. Mice were killed by CO_2 euthanasia upon severe leukocytosis, splenic enlargement and/or moribund appearance. Organs were fixed in 10% neutral buffered formalin and were processed to obtain paraffin sections for histological staining. Bone marrow cells were flushed from tibias and femurs, and spleens were homogenized in IMDM containing 1% BSA. Erythrocytes were then lysed in ACK (150 mM NH_4Cl, 10 mM $KHCO_3$, 0.1 mM EDTA) for 5 min, and nucleated cells were resuspended in IMDM–1% BSA and filtered through a nylon screen (100 μm) to obtain single-cell suspensions. PCR analysis of Cre-mediated recombination was done as described[8], and *Trp53* loss-of-heterozygosity (LOH) analysis was done using *Trp53* genotyping primers as described by Jackson Laboratory. *Trp53* exon-sequencing primers are available from the authors upon request. Whole bone marrow and spleen cells were stained with antibodies to Sca-1 (BioLegend, 108114), Kit (BioLegend, 105826), Mac-1 (BioLegend, 101212), Gr-1 (BioLegend, 108430), B220 (eBioscience, 45-0452-82), Thy1 (BioLegend, 105324), CD3ε (BioLegend, 100222), CD4 (BioLegend, 100428), CD8 (BioLegend, 100725) and Ter-119 (BioLegend, 116232). Flow cytometry was run on an LSR-II or Fortessa flow cytometer (BD Biosciences), and results were analyzed using FACSDiva (BD Biosciences) and FlowJo (Treestar) software.

Phospho-FACS. These procedures were carried out as described previously[8,10]. GM-CSF was used as a stimulation cytokine in the initial mouse model expressing *Kras*^{G12D} with *Trp53* knockdown because of the mature myeloid nature of the leukemia. In experiments involving the *Trp53*$^{+/-}$; *Kras*^{G12D} model with *Spry4* knockdown, serum was used as a broad extrinsic activation medium for the Ras signaling pathway for sarcoma cells with or without the myeloid marker Mac-1. Because of the relatively immature phenotype of *Trp53*$^{-/-}$; sh*Nf1*; sh*Spry4* cells, interleukin 3 (IL-3) was used, as it activates a broader range of cells, including myeloid progenitors and mature myeloid cells. To quantify signaling intensity, we defined the relative mean fluorescence intensity as (mean fluorescence intensity of GFP$^+$ cells)/(mean fluorescence intensity of GFP$^-$ cells) (**Fig. 1b** and **Supplementary Fig. 1a–d**) and as (mean fluorescence intensity with primary antibody)/(mean fluorescence intensity without primary antibody) in cases of dual-fluorescence markers (mCherry and GFP) (**Supplementary Fig. 7b**).

Immunoblot analysis. For comparison of Kras expression, GFP$^+$ *Kras*^{G12D}-only leukemic cells and *Kras*^{G12D} cells with *Trp53* shRNA were sorted and lysed in Laemmli buffer. Equal amounts of protein were separated by 12% SDS-PAGE and transferred to polyvinylidene fluoride membranes. Antibody to Kras (F234, sc-30, Santa Cruz Biotechnology) was used for detecting the amount of total Kras, and the abundance of β-actin was monitored to ensure equal loading. Images were analyzed using AlphaView software (ProteinSimple). For *Spry4* knockdown analysis, NIH 3T3 cells were first infected with an MSCV-5xFlag-Spry4-hygro construct and then selected with hygromycin to generate a stable line expressing Flag-Spry4. These cells were then infected with MLP-based *Spry4* shRNA once for low multiplicity of infection (m.o.i.) and three times for high m.o.i. After selection with puromycin, cells were lysed for protein extraction as described[39]. F1804 monoclonal anti-Flag M2 (Sigma) was used for detecting the expression of Spry4.

Genomic data analysis. Copy number aberrations and chromosome deletions were identified on the basis of available TCGA AML data[1]. Raw data were downloaded from the TCGA Data Portal. Cancer genome data sets and bioinformatics tools for visualizing different parameters for the analysis of genomic data are accessible through the MSKCC cBioPortal (http://www.cbioportal.org/).

doi:10.1038/ng.3251

Copy number states (homozygous deletion, hemizygous deletion, gain and amplification) were determined with the Affymetrix SNP 6.0 platform by the copy number analysis algorithms GISTIC[40] and RAE[41].

Human AML samples were obtained from the University of Chicago. SNP array–based copy number analyses of 35 samples were obtained from published results[42], and data analysis and expression-level estimates were done as described[42]. Gene set enrichment analysis was carried out using the GSEA method with GSEA v2.1.0 (Broad Institute)[43]. Multiple testing–adjusted *P* values (FDR *q* value) less than 0.05 were considered statistically significant.

Statistics and general methods. For mouse survival studies, at least five mice per experimental category were used; for biochemical studies, three mice per group were used. Significant results were subsequently confirmed in independent experiments and are presented in all figures as biological replicates. Mice were housed and used randomly, and the investigators were not blinded for the experiments, with the exception of histopathological analysis. No exclusion of data was carried out, except in cases of overall survival curves, when mice were censored if premature death was caused by non-biological factors (i.e., mice were euthanized for a pre-disease endpoint).

Differences between groups were calculated by *t*-test or ANOVA or with Welch's correction when variance was not similar between groups. Mouse gene suppression was analyzed with Column Statistics. For mouse transplantation experiments, statistical evaluation of overall survival was based on the log-rank (Mantel-Cox) test for comparison of the Kaplan-Meier event-time format. Co-occurrence analyses were derived from the MSKCC cBioPortal or by Fisher's exact test and a permutation test comparing the observed number of co-occurring events with the expected number of co-occurring events under a null distribution generated by 10,000 sample permutations (preexisting).

35. Dickins, R.A. *et al.* Probing tumor phenotypes using stable and regulated synthetic microRNA precursors. *Nat. Genet.* **37**, 1289–1295 (2005).
36. Dow, L.E. *et al.* A pipeline for the generation of shRNA transgenic mice. *Nat. Protoc.* **7**, 374–393 (2012).
37. Fellmann, C. *et al.* An optimized microRNA backbone for effective single-copy RNAi. *Cell Rep.* **5**, 1704–1713 (2013).
38. Schmitt, C.A. *et al.* Dissecting p53 tumor suppressor functions *in vivo*. *Cancer Cell* **1**, 289–298 (2002).
39. Hemann, M.T. *et al.* An epi-allelic series of p53 hypomorphs created by stable RNAi produces distinct tumor phenotypes *in vivo*. *Nat. Genet.* **33**, 396–400 (2003).
40. Mermel, C.H. *et al.* GISTIC2.0 facilitates sensitive and confident localization of the targets of focal somatic copy-number alteration in human cancers. *Genome Biol.* **12**, R41 (2011).
41. Taylor, B.S. *et al.* Functional copy-number alterations in cancer. *PLoS One* **11**, e3179 (2008).
42. McNerney, M.E. *et al. CUX1* is a haploinsufficient tumor suppressor gene on chromosome 7 frequently inactivated in acute myeloid leukemia. *Blood* **121**, 975–983 (2013).
43. Subramanian, A. *et al.* Gene set enrichment analysis: a knowledge-based approach for interpreting genome-wide expression levels. *Proc. Natl. Acad. Sci. USA* **102**, 15545–15550 (2005).